

# From Thermogelling Hydrogels toward Functional Bioinks: Controlled Modification and Cytocompatible Crosslinking

Lukas Hahn, Matthias Beudert, Marcus Gutmann, Larissa Keßler, Philipp Stahlhut, Lena Fischer, Emine Karakaya, Thomas Lorson, Ingo Thievensen, Rainer Detsch, Tessa Lühmann,\* and Robert Luxenhofer\*

Hydrogels are key components in bioink formulations to ensure printability and stability in biofabrication. In this study, a well-known Diels-Alder two-step post-polymerization modification approach is introduced into thermogelling diblock copolymers, comprising poly(2-methyl-2-oxazoline) and thermoresponsive poly(2-*n*-propyl-2-oxazine). The diblock copolymers are partially hydrolyzed and subsequently modified by acid/amine coupling with furan and maleimide moieties. While the thermogelling and shear-thinning properties allow excellent printability, trigger-less cell-friendly Diels-Alder click-chemistry yields long-term shape-fidelity. The introduced platform enables easy incorporation of cell-binding moieties (RGD-peptide) for cellular interaction. The hydrogel is functionalized with RGD-peptides using thiol-maleimide chemistry and cell proliferation as well as morphology of fibroblasts seeded on top of the hydrogels confirm the cell adhesion facilitated by the peptides. Finally, bioink formulations are tested for biocompatibility by incorporating fibroblasts homogeneously inside the polymer solution pre-printing. After the printing and crosslinking process good cytocompatibility is confirmed. The established bioink system combines a two-step approach by physical precursor gelation followed by an additional chemical stabilization, offering a broad versatility for further biomechanical adaptation or bioresponsive peptide modification.

## 1. Introduction

In the field of biofabrication, researchers try to create functional tissue models by using an additive manufacturing technique. Especially in bioprinting, advances strongly rely on the availability of suitable bioinks.<sup>[1–3]</sup> These materials, in turn, are mostly based on polymers—either of synthetic or natural origin—and contain living cells, the required growth factors, as well as nutrition to be processed by an automated biofabrication technology.<sup>[4,5]</sup> In most cases, direct ink-writing of a hydrogel is used, allowing the production of clinically relevant designs with respect to time and size.<sup>[6]</sup> Bioinks have to be printable at cell friendly conditions, and allow maturation of the printed construct for several weeks. Several key characteristics can be associated with an ideal hydrogel bioink. First, a pronounced shear thinning character of the precursor hydrogel during extrusion facilitates 3D-printing and concurrently the viscoelastic solid like character prevents cell sedimentation in the barrel.<sup>[7]</sup> Second, it

L. Hahn, L. Keßler, R. Luxenhofer  
Functional Polymer Materials, Chair for Advanced Materials Synthesis,  
Institute for Functional Materials and Biofabrication, Department of  
Chemistry and Pharmacy and Bavarian Polymer Institute  
Julius-Maximilians-University Würzburg  
Röntgenring 11, Würzburg 97070, Germany  
E-mail: robert.luxenhofer@helsinki.fi

M. Beudert, M. Gutmann, T. Lorson, T. Lühmann  
Institute of Pharmacy and Food Chemistry  
Julius-Maximilians-University Würzburg  
Am Hubland, Würzburg 97074, Germany  
E-mail: tessa.luehmann@uni-wuerzburg.de

P. Stahlhut  
Department for Functional Materials in Medicine and Dentistry  
University of Würzburg  
Pleicherwall 2, Würzburg 97070, Germany

L. Fischer, I. Thievensen  
Center for Medical Physics and Technology, Biophysics Group  
Friedrich-Alexander-University of Erlangen-Nuremberg  
Henkestrasse 91, Erlangen 91052, Germany

E. Karakaya, R. Detsch  
Institute of Biomaterials  
University of Erlangen-Nürnberg  
Cauerstr. 6, Erlangen 91058, Germany

R. Luxenhofer  
Soft Matter Chemistry, Department of Chemistry and Helsinki Institute  
of Sustainability Science, Faculty of Science  
University of Helsinki  
P.O. Box 55, Helsinki FIN-00014, Finland

 The ORCID identification number(s) for the author(s) of this article can be found under <https://doi.org/10.1002/mabi.202100122>

© 2021 The Authors. Macromolecular Bioscience published by Wiley-VCH GmbH. This is an open access article under the terms of the Creative Commons Attribution-NonCommercial-NoDerivs License, which permits use and distribution in any medium, provided the original work is properly cited, the use is non-commercial and no modifications or adaptations are made.

DOI: 10.1002/mabi.202100122

should ideally allow for sufficient and fast stabilization after the printing process. The former, that is, the formation of a precursor hydrogel, can be ensured by a wide variety of approaches, such as specific chemical pre-crosslinking,<sup>[8]</sup> pH,<sup>[9]</sup> or temperature switch,<sup>[10]</sup> as described, for example, for alginate, collagen, and gelatine. The defined control of these approaches to provide a cytocompatible printing process is an ongoing challenge.

Thermogelling polymer solutions that undergo fast gelation are promising candidates for bioinks. A well-known example is the polymer Pluronic F127, also known as Poloxamer 407. This triblock copolymer based on polypropylene glycol as thermoresponsive central block, flanked by two hydrophilic polyethylene glycol (PEG) blocks, forms a physical hydrogel at room temperature. Since Pluronic F127 gels represent excellent printability,<sup>[11]</sup> they are used in many applications as a support material and sacrificial structure.<sup>[12]</sup> One possible alternative for PEG-based systems is the family of polymers known as poly(2-oxazoline)s (POx) and their close relative poly(2-substituted-5,6-dihydro-4H-1,3-oxazine)s (poly(2-oxazine)s, POzi), which serve as a diverse biomaterials platform for different applications due to good cytocompatibility and chemical versatility.<sup>[13–17]</sup>

In the context of biofabrication, only few reports can be found describing POx/POzi based structures used in bioprinting. Lorton et al. reported a thermogelling diblock copolymer comprising hydrophilic poly(2-methyl-2-oxazoline) (PMeOx) and thermoresponsive poly(2-*n*-propyl-2-oxazine) (P*n*PrOzi) moieties.<sup>[18]</sup> In first bioprinting experiments excellent cytocompatibility was confirmed. The printability and shape fidelity could be significantly improved by the addition of Laponite XLG.<sup>[19]</sup> However, this thermoresponsive hydrogel does not allow for long-term cell culture experiments, as it dissolves upon addition of an excess of cell culture medium. More recently, Trachsel et al. investigated a multi-material approach with enzymatically stabilized hydrophilic poly(2-ethyl-2-oxazoline) hydrogels via sortase linkage.<sup>[20]</sup> To use this system in a bioink formulation, alginate was needed to stabilize the constructs after printing by Ca<sup>2+</sup>. Furthermore, cellulose nanofibrils were added to improve printability.<sup>[21]</sup>

In recent years, several approaches—mainly based on irradiation with UV-light—have been described to introduce covalent crosslinking after printing,<sup>[22–24]</sup> fueling ongoing and controversial discussions about the potential negative effect of UV irradiation on cell viability.<sup>[24,25]</sup> More recently, crosslinking using visible light has gained attention. Irrespective of the wavelength used, photoinitiators are typically needed for crosslinking which may affect cells either immediately or during the maturation.<sup>[24]</sup> Accordingly, alternative approaches of in situ chemical crosslinking of hydrophilic polymers by the reaction of complementary functional groups, to obtain hydrogels, remain actively investigated. One such alternative is the Diels-Alder chemistry, already introduced for hydrogel synthesis by Chujo et al. a few decades ago<sup>[26]</sup> besides other crosslinking strategies<sup>[27,28]</sup> and recently studied again by Shoichet et al.<sup>[29–32]</sup> as well as Nahm et al.,<sup>[33]</sup> among others. Chujo et al. used the hydrophilic PMeOx functionalized with maleimide and furan groups in the polymer side chain. However, these hydrogel precursors would be unlikely candidates for dispense plotting, due to their hydrophilic nature and expected rheological properties.

In this work, we established a double-crosslinked bioink platform obtained by one starting block copolymer and its modifications, combining thermoresponsive precursor gelation together with temperature-controlled Diels-Alder crosslinking, in order to employ the benefits of both crosslinking mechanisms for creating a functional and adaptable bioink platform. Therefore, a previously described diblock copolymer comprising a hydrophilic PMeOx block and a thermoresponsive P*n*PrOzi block (PMeOx-*b*-P*n*PrOzi = P0),<sup>[18]</sup> which showed pronounced physical thermogelation in aqueous solutions, was modified with furan and maleimide moieties.<sup>[26]</sup> The fast physical sol/gel transition was used to obtain a homogenous cell distribution throughout the construct, in combination with good printability. After the extrusion, the cytocompatible in situ Diels-Alder crosslinking stabilized the construct and offered the possibility to introduce bioinstructive peptides. Beside the two functionalized polymers, no further compound such as crosslinker, initiators or viscosity modulators were used in order to obtain both a physically and chemically crosslinked hydrogel.

## 2. Results and Discussion

The presented bioink concept builds on two independent crosslinking mechanisms. At first, thermoreversible hydrophobic interactions offer excellent handling and printing properties. Second, a slow but essentially irreversible Diels-Alder crosslinking post-processing provides long-term stability and maturation.

In addition, Diels-Alder functionalities enable the conjugation of bioactive components (**Figure 1A**).<sup>[34–36]</sup> In order to introduce the corresponding functionalities, the thermogelling diblock copolymer P0, with a similar degree of polymerization as described previously,<sup>[18]</sup> was partially hydrolyzed, yielding secondary amines, which are subsequently coupled with carboxylic acids (**Figure 1B**). Doing so, it is critical that the thermogelling properties of the polymer P0 (**Figure S1**, Supporting Information) are retained after modification and that the crosslinking occurs in a time period suitable for bioprinting. The first step was a carefully controlled partial hydrolysis of the polymer yielding ethyleneimine (EI) moieties in the hydrophilic part of the polymer. We expected that the MeOx repeat units are hydrolyzed significantly faster than the *n*PrOzi units.<sup>[37,38]</sup> <sup>1</sup>H-Nuclear magnetic resonance (NMR) spectroscopy confirmed that backbone and sidechain signals attributed to MeOx repeat units decreased significantly with increasing reaction time (**Figures S2, S3A, B**, Supporting Information), while the signals attributed to *n*PrOzi repeat units remained preserved. The degree of hydrolysis has a significant impact on the thermogelling properties (**Figure S3C**, Supporting Information). Here, the polymers with a hydrolysis degree of 10% of the PMeOx block were further investigated ((P(MeOx<sub>90-co</sub>-EI<sub>10</sub>)-*b*-P*n*PrOzi<sub>100</sub> = P1). The thermogelling properties of three different P1 polymer batches performed similar like the unmodified polymers described by Lorton et al. (**Table S1**, Supporting Information),<sup>[18]</sup> indicating the reproducibility of the approach.<sup>[39]</sup> Modification of P1 with furan or maleimide moieties resulted in the final functionalized polymers P(MeOx<sub>90-co</sub>-Fu<sub>10</sub>)-*b*-P*n*PrOzi<sub>100</sub> (P-Fu) and P(MeOx<sub>90-co</sub>-Ma<sub>10</sub>)-*b*-P*n*PrOzi<sub>100</sub> (P-Ma). The successful and complete modification was verified by <sup>1</sup>H-NMR spectroscopy (**Figure S4**, Supporting Information) and

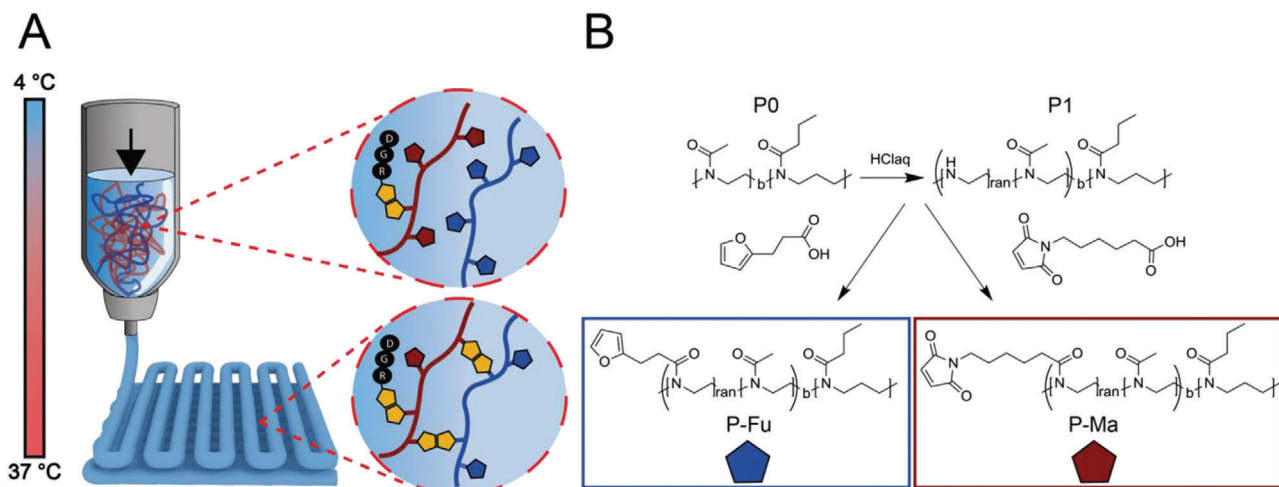


**Figure 1.** Investigated strategy for functional bioink formulations. A) Schematic illustration of the bioink strategy. At 5 °C the polymer solutions P-Fu and P-Ma are present as low viscous liquids, which can be easily mixed with cells and peptide motifs (e.g., RGD). Increasing the temperature to 37 °C leads to a rapid physical gelation of both P-Fu and P-Ma preventing cell sedimentation and ensuring good printability. After printing, the chemical crosslinking takes place at 37 °C generating stable and biofunctionalized constructs. B) Synthesis route to establish the thermogelling polymers P-Fu and P-Ma: Partial acidic hydrolysis of the thermogelling diblock copolymer P0 followed by the introduction of furan and maleimide moieties by amide coupling (P-Fu and P-Ma).

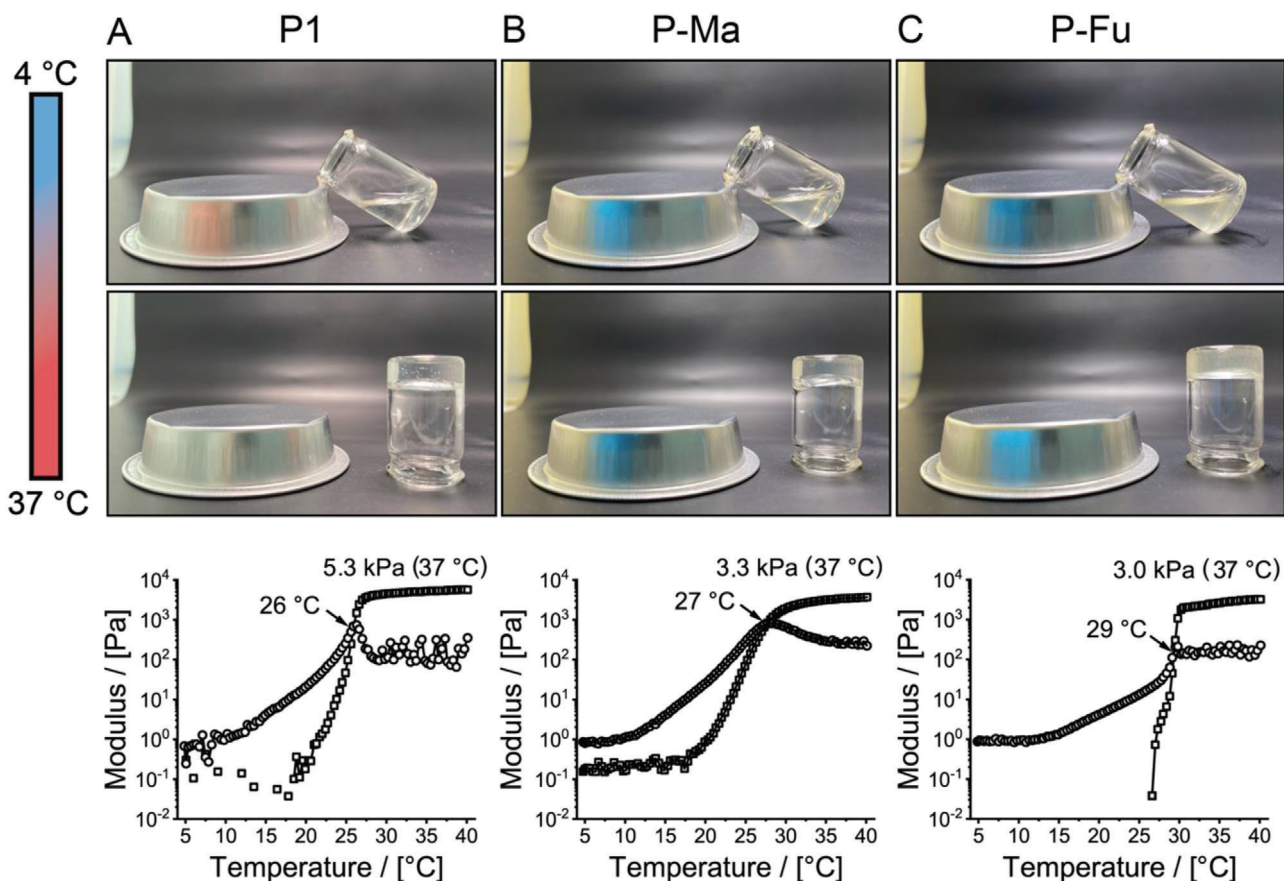


**Figure 2.** Thermogelling properties of the different modified polymers. A) P1, B) P-Ma, and C) P-Fu in the temperature range of 5–37 °C (heat rate: 0.05 °C s<sup>-1</sup>) and at 20 wt% aqueous solutions (□: Storage modulus  $G'$ , ○: Loss modulus  $G''$ ). Images were taken at 5 and 37 °C following the described temperature scale.

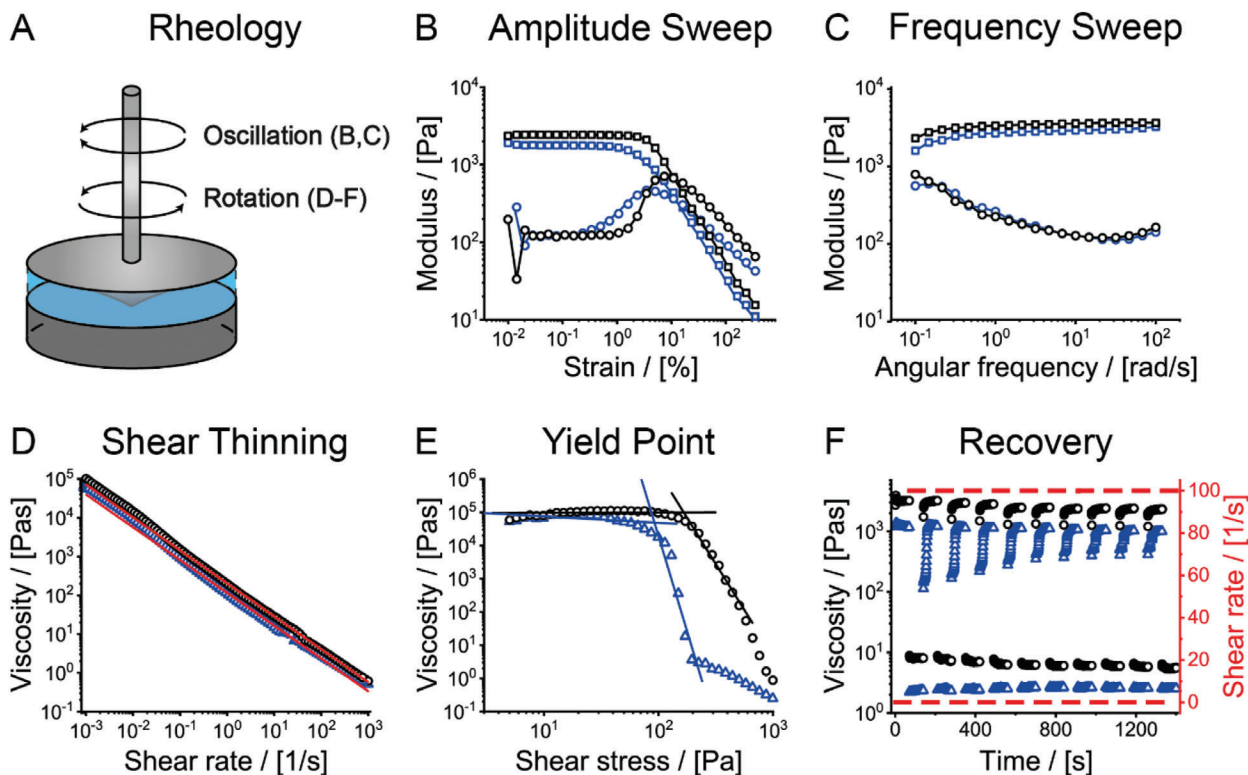


**Figure 3.** Determination of important rheological properties. A) Rheological properties for direct ink-writing of P-Fu (blue) and P-Ma (black) at a concentration of 20 wt% and 37 °C. B) Amplitude sweep ( $\square$ : Storage modulus  $G'$ ,  $\circ$ : Loss modulus  $G''$ ) and C) frequency sweep. D) Shear thinning properties: Viscosity in dependence of the applied shear rate. Red line: data fitted with a power law function. E) Yield point determination: Viscosity as a function of applied shear stress. The onset of viscosity decrease designates the yield point  $\tau$ . F) Structure-recovery properties: Alternated high and low-shear regimes.

all relevant signals could be attributed. It is important to note that the signals attributed to EI repeat units completely disappeared. Furthermore, complete modification of all secondary amines (EI units) was confirmed via titration (Figure S4, Supporting Information).

The polymers P1, P-Fu and P-Ma exhibited pronounced thermogelling properties in the temperature range of 5–40 °C (5 °C low viscous liquid, 40 °C stable hydrogel, Figure 2) with sol/gel transitions between 26 and 29 °C (Figure 2). Compared to the precursor polymer P0 the transition temperature increased, which simplifies handling at room temperature ( $T_{\text{gel}}$  (P0) = 21 °C, Figure S1, Supporting Information). Notably, the storage modulus  $G'$  at 37 °C increased from 3.8 kPa for P0 to 5.3 kPa for P1 (Figure 2A). In contrast, the addition of furan and maleimide moieties resulted to a reversal of  $G'$  to 3.3 and 3.0 kPa, respectively (Figure 2B,C). Clearly, modifications of the hydrophilic block affect the polymer self-assembly, presumably by affecting the compatibility between the blocks. The physical hydrogels P-Fu and P-Ma at 37 °C and a concentration of 20 wt% were further characterized individually via oscillatory and rotational shear rheology to investigate whether their rheological parameters would be favorable for 3D printing (Figure 3).

Both samples showed a pronounced linear viscoelastic region in the amplitude sweep (Figure 3B). Slightly higher  $G'$  values are obtained for the polymer P-Ma, which is in agreement with the values obtained during the temperature sweep (Figure 2). In the

investigated frequency region both polymers exhibited viscoelastic solid-like character throughout (Figure 3C). The pronounced shear-thinning (Figure 3D) with flow indices of  $n = 0.15$  for P-Fu and P-Ma, well-defined yield-points (Figure 3E;  $\tau$  (P-Fu) = 92 Pa and  $\tau$  (P-Ma) = 166 Pa), high viscosity at low shear stress ( $\approx 100$  kPa s) and fast structure recovery (Figure 3F) suggests good printability for both hydrogels. This rheological profile allows the low viscosity polymer sols to be mixed with cells at  $\leq 10$  °C, and subsequently printed at 37 °C on a preheated printing dish, where the crosslinking Diels-Alder reaction takes place, subsequently (Figure 4A).

Accordingly, we mixed 20 wt% aqueous solutions of both polymers (1/1, v/v) at 10 °C and followed  $G'$  and  $G''$  at 10, 20, and 37 °C over time (Figure 4B). Over the investigated time of 2 h no hydrogel formation was observed at 10 °C and the sample remained a low viscous liquid, ideal for sample preparation, cell distribution, and transfer into a printing syringe. Only a minor increase in viscosity is observed after  $\approx 1$  h. With a temperature-controlled printing setup, this allows for prolonged printability, if needed. In contrast, at 25 °C, which is below  $T_{\text{gel}}$  hydrogel, a sol/gel transition is observed after 65 min and must be attributed to the Diels-Alder crosslinking. At 37 °C the mixture thermogelled immediately, followed by additional Diels-Alder crosslinking, as evidenced by an increase of  $G'$  and  $G''$ . After less than 50 min a plateau value of more than 10 kPa was reached. Accordingly, printing the bioink at room temperature onto a preheated

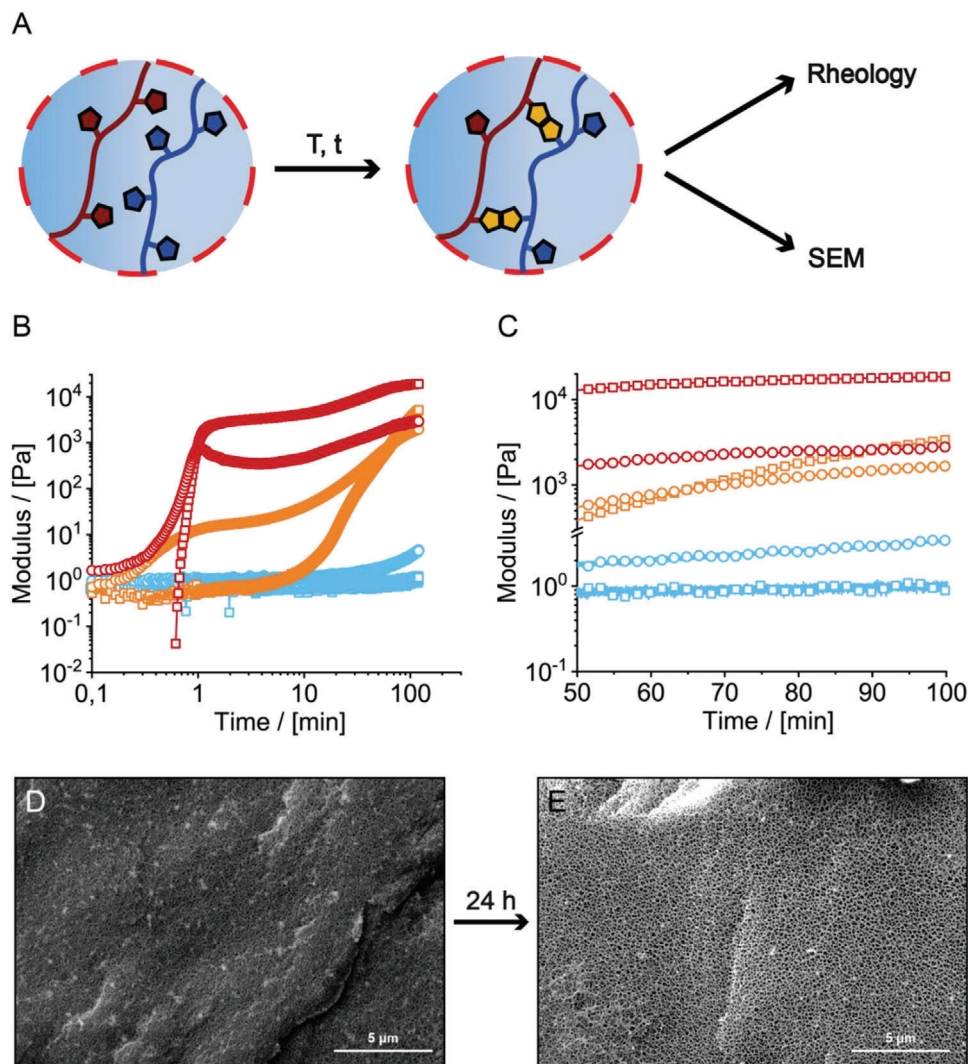


**Figure 4.** Chemical crosslinking of mixed P-Fu and P-Ma hydrogels. A) Workflow for crosslinking analysis (B–C) Crosslinking kinetics of P-Fu and P-Ma mixtures (1:1) at different temperatures (blue: 10 °C, orange: 20 °C, and red: 37 °C) and 20 wt% concentration ( $\square$ : Storage modulus  $G'$ ,  $\circ$ : Loss modulus  $G''$ ): B) Time scans of 120 min with a fixed amplitude of 0.5 % and an angular frequency of 10 rad s<sup>-1</sup> with a C) detailed view for 50–100 min which we deem critical for preparing and conducting a typical print. Cryogenic scanning electron microscopy (SEM) investigations to visualize the porous structure of the bioink: Samples were recorded after D) crosslinking of 24 h and E) additional swelling for 24 h.

dish should ensure rapid crosslinking and stability of the printed construct.

Due to the nature of the chemical crosslinked synthetic hydrogel, a highly porous network with features in the range of a few dozen nm was obtained (Figure 4D). Swelling for 24 h led to a significant increase in pore size into the lower 100 nm range (Figure 4E). Although the pore size is sufficiently large for diffusion of nutrients, cells will not be able to migrate through the generated network. Compared to the physical hydrogel of P0 (Figure S1B, Supporting Information) the pore size decreased significantly after chemical crosslinking, due to the formation of a more compact three-dimensional covalent network. In order to highlight the adaptability of the platform in terms of stiffness, the concentration of precursor solutions of P-Fu and P-Ma was decreased by dilution with water leading to softer hydrogels with slower crosslinking kinetics (Figure S5, Supporting Information). Ad-

ditionally, the nature of the crosslinker can be adapted to specific applications. To demonstrate this, we used PEG<sub>600</sub>-bismaleimide as a model crosslinker. The P-Fu-PEG mixtures showed a slower crosslinking and resulted in softer and less dense networks as characterized by rheology and cryogenic scanning electron microscopy, respectively (Figure S6, Supporting Information). Not surprising, this led to a more pronounced swelling of the hydrogels compared to the P-Fu/P-Ma crosslinking.

Based on the favorable rheological properties of the precursor hydrogels and the controlled crosslinking kinetics, first 3D printing experiments were performed. At 5 °C, P-Fu and P-Ma solutions were homogeneously mixed and transferred into a printing cartridge (held at 5 °C) followed by printing onto a preheated (37 °C) printing bed (Figure 5A–C). After 1 h of in situ chemical crosslinking at 37 °C, the constructs were immersed in fresh cell culture medium and incubated for 14 days at 37 °C. The

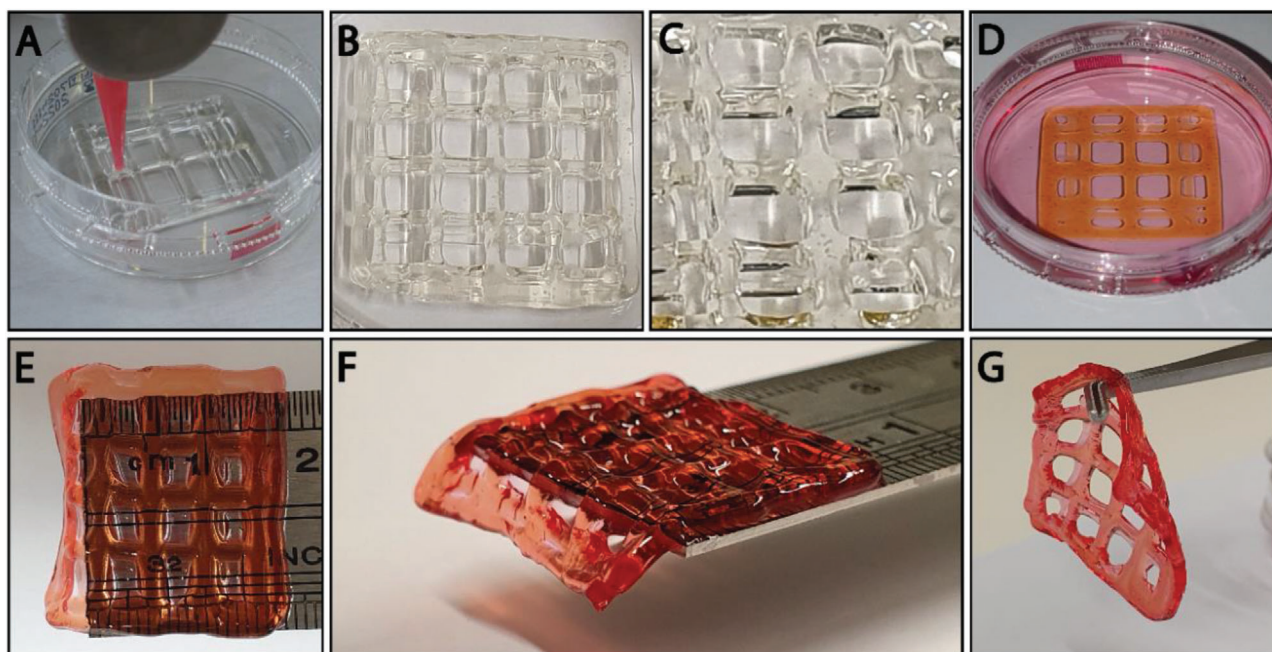


**Figure 5.** Printing of P-Fu and P-Ma crosslinking hydrogels. A) Image of the printed scaffold during the printing process. B,C) Illustration of the printed scaffold immediately after printing. D) Printed scaffolds after incubation in culture medium for 14 days. E–G) Handling and transfer of P-Fu and P-Ma crosslinked hydrogels after 14 days in culture medium.

constructs remained stable with good structural integrity (Figure 5D). However, fusion of stacked layers with direct contact can be seen. During incubation, swelling increases the contact between individual layers, which can then cross-link with each other. In the end, this leads to a homogeneous construct with relatively low stackability. Even though the hydrogels are soft, as analyzed by rheology and shown above, they were easily handled and transferred while retaining their printed shape (Figure 5D–G).

Furthermore, we analyzed the swelling of the crosslinked P-Fu and P-Ma hydrogels (20 wt%, ratio P-Fu/P-Ma 1:1). Only little swelling was observed (Figure S10A, Supporting Information), which is explained by the combination of physical and chemical crosslinking with several crosslinking functionalities at every polymer molecule. Interestingly, a significant increase of swelling was observed at 5 °C (Figure S10C,D, Supporting Information). Below the lower critical solution temperature of the nPrOzi block the swelling of the hydrogel increased significantly due to an increased solubility of the thermoresponsive nPrOzi block and the removal of physical crosslinks upon cooling. In addition, the stability was further confirmed by mechanical testing. Elastic moduli of approximately 3000–4000 kPa were obtained for the crosslinked hydrogels after 14 days (Figure S10B, Supporting Information).

As mentioned above, it has been shown that different POx-based hydrogels show no cytotoxic effects on cells and therefore present a promising platform for bioinks.<sup>[40–44]</sup> However, applicability in biomedicine requires the adhesive functionalization of POx-based hydrogels, as the material per se does not support cell adhesion. To test, whether adhesive functionalization of our hydrogels supports cell adhesion, we functionalized them with integrin-ligating RGD-peptide. We further generated lentivirally transduced, NIH/3T3-based morphology reporter cells, stably ex-

pressing farnesylated tdTomato red-fluorescent protein, to label the plasma membrane and compared the morphology of our reporter cells cultured on top of RGD-functionalized and non-functionalized POx hydrogels. Epifluorescence microscopy analysis after 3 and 4 days of cultivation revealed that cells on non-functionalized POx hydrogels were low in number and showed a rounded morphology (Figure 6A,C), whereas cells on RGD-functionalized hydrogels displayed a well spread fibroblastoid morphology (Figure 6B) and even increased in number over time (Figure 6D). These data demonstrate that adhesive functionalization of our POx hydrogels supports cell adhesion, spreading and proliferation.

To further study cell viability within the gel (3D), NIH3T3 cells were embedded in the hydrogel pre-printing. After the printing process and cross-linking of the hydrogels, the cell viability of the encapsulated cells in the scaffold was analyzed. Cells were pre-stained with Hoechst 33342 prior to the printing process. This was necessary as preliminary work showed that fluorescein diacetate (FDA) was not able to penetrate the gels in a sufficient manner. Dead cells were visualized using propidium iodide (PI) (here no incompatibilities with in-gel penetration where observed) staining after 1 and 2 days. After optimizing the polymer purification process (Figure S8, Supporting Information) as well as the printing protocol, cell viability staining showed no cytotoxic effect of the hydrogel. No difference between the unmodified and RGD-functionalized constructs was observed. The majority of dead cells that were visible, scanning the entire printed hydrogel construct, could be accounted to drying-off effects at the outer layers, which was reported for other hydrogel systems before (Figure S9, Supporting Information).<sup>[45,46]</sup> Despite the RGD-functionalization, the cells showed a rounded morphology after the encapsulation in the hydrogel (Figure 7). It

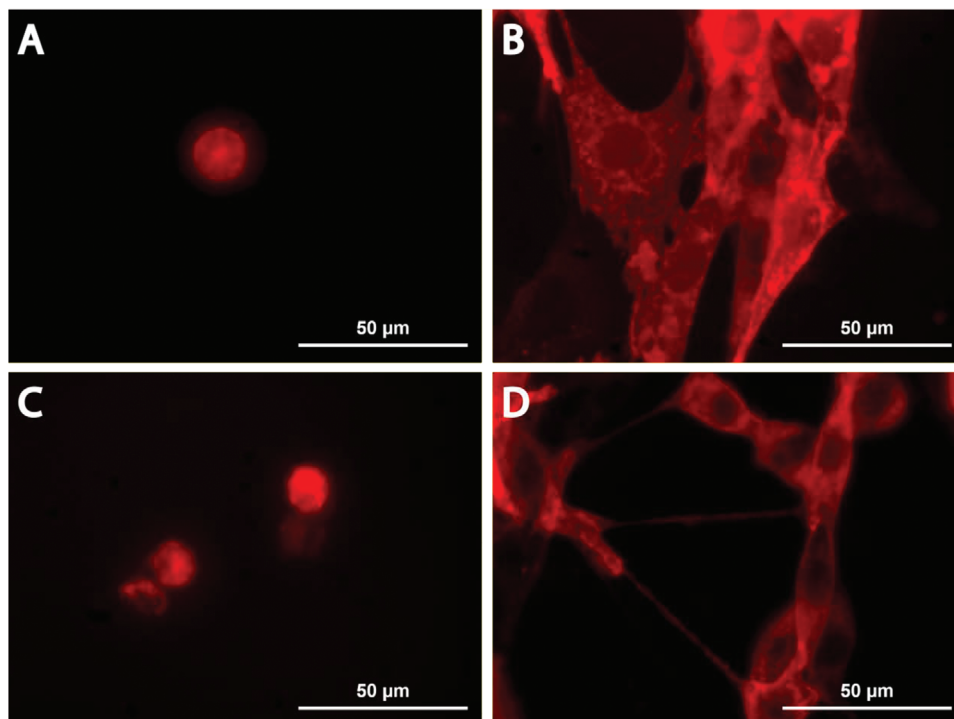


**Figure 6.** Cell adhesion on the surface of P-Fu and P-Ma crosslinking hydrogels. POx hydrogel without RGD-modification does not allow for good cell adhesion and spreading after A) 3 and C) 4 days. In contrast, cell adhesion and spreading were observed on POx hydrogel with RGD-modification after B) 3 days of and D) 4 days of cultivation.

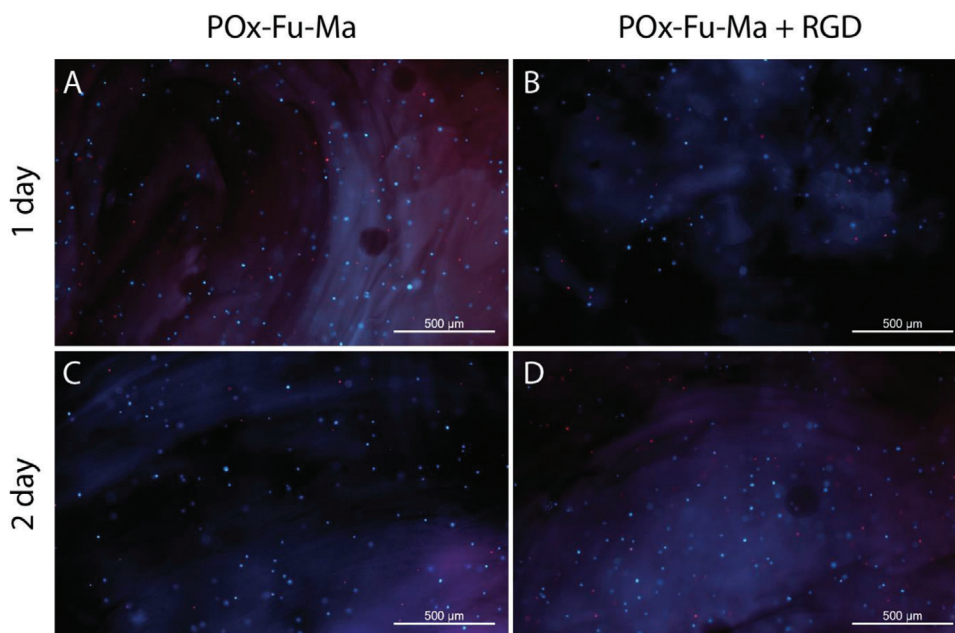


**Figure 7.** Cell viability of fibroblasts in P-Fu/P-Ma-bioinks after deposition of a bioink drop by extrusion printing. NIH3T3 cells were pre-stained with Hoechst 33342 (blue) and incorporated, printed, and cultivated in POx-based hydrogels (20 wt%) B,D) with and A,C) without RGD-peptide. Dead cells were assessed by staining with PI (red).

has been previously described that POx hydrogels with moduli of around of around 3.5–4.5 kPa are too stiff for the migration of the cells.<sup>[47,48]</sup> Furthermore, small pore sizes, as described above for this system, have been shown to prevent cell spreading and migration.<sup>[49,50]</sup> With  $G'$  of around 10 kPa and submicron pore size, the hydrogel system, as shown in this study, clearly does not allow the migration and therefore the spreading of the cells.

In an effort to address cell adhesion and migration, we aim at incorporating matrix metalloprotease (MMP) cleavable linkers into the hydrogel network, to ensure cleavage by secreted MMPs and therefore a loosening of the network as demonstrated before.<sup>[51–53]</sup> The sequence of the linker (GPQGIAGQ) is derived from collagen. It has been shown to be responsive to MMP cleavage and has already been used in different applications.<sup>[54–57]</sup> The linker can be flanked with either thiol or maleimide groups for the cross-linking of both P-Fu and P-Ma and is part of the ongoing research.

### 3. Conclusion

In this study, favorable thermogelation and shear-thinning properties were combined with cell friendly post-printing chemical crosslinking via Diels-Alder chemistry. The post-polymerization modification preserved the nature of physical crosslinked hydrogels. The crosslinking kinetics and density could be fine-tuned with different temperatures and crosslinking degrees. The second crosslinking step ensured stability of printed constructs over at least two weeks. Biofunctionality was introduced via the attachment of RGD binding motives and NIH 3T3 cells showed cell adhesion and an elongated morphology, when seeded on top of the hydrogels for a couple of days. First bioprinting experiments highlighted the optimized printing setup, the biocompatibility and the functionality of the investigated bioink formulation. With this study, we demonstrate a dual-gelling system based on the versatile and cytocompatible polymer classes of POx and POzi that was used to develop a functional bioinks. Furthermore, the platform can be conveniently decorated with biofunctionalities, which makes it adaptable for many specific applications.

### Supporting Information

Supporting Information is available from the Wiley Online Library or from the author.

### Acknowledgements

L.H. and M.B. contributed equally to this work. The authors would like to gratefully acknowledge support by the Deutsche Forschungsgemeinschaft (DFG, German Research Foundation)-project number 326998133-TRR225 (subprojects A03, B06). Furthermore, the authors thank the Deutsche Forschungsgemeinschaft for funding the crossbeam scanning electron microscope Zeiss CB 340 (INST 105022/58-1 FUGG) within the DFG State Major Instrumentation Programme.

Open access funding enabled and organized by Projekt DEAL.

### Conflict of Interest

The authors declare no conflict of interest.

### Data Availability Statement

The data that support the findings of this study are available from the corresponding author upon reasonable request.

### Keywords

biofabrication, bioprinting, chemical crosslinking, hydrogels

Received: March 25, 2021

Revised: June 20, 2021

Published online: July 22, 2021

- [1] L. Moroni, T. Boland, J. A. Burdick, C. De Maria, B. Derby, G. Forgacs, J. Groll, Q. Li, J. Malda, V. A. Mironov, C. Mota, M. Nakamura, W. Shu, S. Takeuchi, T. B. F. Woodfield, T. Xu, J. J. Yoo, G. Vozzi, *Trends Biotechnol.* **2018**, *36*, 384.
- [2] D. Chimene, K. K. Lennox, R. R. Kaunas, A. K. Gaharwar, *Ann. Biomed. Eng.* **2016**, *44*, 2090.
- [3] L. Valot, J. Martinez, A. Mehdi, G. Subra, *Chem. Soc. Rev.* **2019**, *48*, 4049.
- [4] J. Groll, J. A. Burdick, D. - W. Cho, B. Derby, M. Gelinsky, S. C. Heilshorn, T. Jüngst, J. Malda, V. A. Mironov, K. Nakayama, A. Ovsianikov, W. Sun, S. Takeuchi, J. J. Yoo, T. B. F. Woodfield, *Biofabrication* **2018**, *11*, 013001.
- [5] J. Groll, T. Boland, T. Blunk, J. A. Burdick, D.-W. Cho, P. D. Dalton, B. Derby, G. Forgacs, Q. Li, V. A. Mironov, L. Moroni, M. Nakamura, W. Shu, S. Takeuchi, G. Vozzi, T. B. F. Woodfield, T. Xu, J. J. Yoo, J. Malda, *Biofabrication* **2016**, *8*, 013001.
- [6] D. Chimene, R. Kaunas, A. K. Gaharwar, *Adv. Mater.* **2020**, *32*, 1902026.
- [7] T. Jüngst, W. Smolan, K. Schacht, T. Scheibel, J. Groll, *Chem. Rev.* **2016**, *116*, 1496.
- [8] J. Hazur, R. Detsch, E. Karakaya, J. Kaschta, J. Teßmar, D. Schneiderreit, O. Friedrich, D. W. Schubert, A. R. Boccaccini, *Biofabrication* **2020**, *12*, 045004.
- [9] E. O. Osidak, V. I. Kozhukhov, M. S. Osidak, S. P. Domogatsky, *Int. J. Bioprint.* **2020**, *6*, 270.
- [10] L. Ouyang, R. Yao, Y. u Zhao, W. Sun, *Biofabrication* **2016**, *8*, 035020.
- [11] M. Müller, J. Becher, M. Schnabelrauch, M. Zenobi-Wong, *Biofabrication* **2015**, *7*, 035006.
- [12] D. B. Kolesky, R. L. Truby, A. S. Gladman, T. A. Busbee, K. A. Homan, J. A. Lewis, *Adv. Mater.* **2014**, *26*, 3124.
- [13] T. Lorson, M. M. Lübtow, E. Wegener, M. S. Haider, S. Borova, D. Nahm, R. Jordan, M. Sokolski-Papkov, A. V. Kabanov, R. Luxenhofer, *Biomaterials* **2018**, *178*, 204.
- [14] J. - R. Park, E. C. L. Bolle, A. D. Santos Cavalcanti, A. Podevyn, J. F. R. Van Guyse, A. Forget, R. Hoogenboom, T. R. Dargaville, *Biointerphases* **2021**, *16*, 011001.
- [15] M. M. Lübtow, T. Lorson, T. Finger, F. - K. Gröber-Becker, R. Luxenhofer, *Macromol. Chem. Phys.* **2020**, *221*, 1900341.
- [16] M. M. Lübtow, S. Oerter, S. Quader, E. Jeanclos, A. Cubukova, M. Krafft, M. S. Haider, C. Schulte, L. Meier, M. Rist, O. Sampetean, H. Kinoh, A. Gohla, K. Kataoka, A. Appelt-Menzel, R. Luxenhofer, *Mol. Pharmaceutics* **2020**, *17*, 1835.
- [17] J. Humphries, D. Pizzi, S. E. Sonderegger, N. L. Fletcher, Z. H. Houston, C. A. Bell, K. Kempe, K. J. Thurecht, *Biomacromolecules* **2020**, *21*, 3318.
- [18] T. Lorson, S. Jaksch, M. M. Lübtow, T. Jüngst, J. Groll, T. Lühmann, R. Luxenhofer, *Biomacromolecules* **2017**, *18*, 2161.
- [19] C. Hu, L. Hahn, M. Yang, A. Altmann, P. Stahlhut, J. Groll, R. Luxenhofer, *J. Mater. Sci.* **2021**, *56*, 691.

- [20] L. Trachsel, N. Broguiere, J. - G. Rosenboom, M. Zenobi-Wong, E. M. Benetti, *J. Mater. Chem. B* **2018**, *6*, 7568.
- [21] L. Trachsel, C. Johnbosco, T. Lang, E. M. Benetti, M. Zenobi-Wong, *Biomacromolecules* **2019**, *20*, 4502.
- [22] S. Stichter, T. Jungst, M. Schamel, I. Zilkowski, M. Kuhlmann, T. Böck, T. Blunk, J. Teßmar, J. Groll, *Ann. Biomed. Eng.* **2017**, *45*, 273.
- [23] S. Bertlein, G. Brown, K. S. Lim, T. Jungst, T. Boeck, T. Blunk, J. Tessmar, G. J. Hooper, T. B. F. Woodfield, J. Groll, *Adv. Mater.* **2017**, *29*, 1703404.
- [24] K. S. Lim, B. S. Schon, N. V. Mekhileri, G. C. J. Brown, C. M. Chia, S. Prabakar, G. J. Hooper, T. B. F. Woodfield, *ACS Biomater. Sci. Eng.* **2016**, *2*, 1752.
- [25] W. T. Han, T. Jang, S. Chen, L. S. H. Chong, H.-D.o Jung, J. Song, *Biomater. Sci.* **2020**, *8*, 450.
- [26] Y. Chujo, K. Sada, T. Saegusa, *Macromolecules* **1990**, *23*, 2636.
- [27] Y. Chujo, K. Sada, T. Saegusa, *Macromolecules* **1990**, *23*, 2693.
- [28] Y. Chujo, K. Sada, T. Saegusa, *Polymer Journal* **1993**, *25*, 599.
- [29] C. M. Nimmo, S. C. Owen, M. S. Shoichet, *Biomacromolecules* **2011**, *12*, 824.
- [30] A. E. G. Baker, R. Y. Tam, M. S. Shoichet, *Biomacromolecules* **2017**, *18*, 4373.
- [31] L. J. Smith, S. M. Taimoory, R. Y. Tam, A. E. G. Baker, N. Binth Mohammad, J. F. Trant, M. S. Shoichet, *Biomacromolecules* **2018**, *19*, 926.
- [32] V. Delplace, P. E. B. Nickerson, A. Ortin-Martinez, A. E. G. Baker, V. A. Wallace, M. S. Shoichet, *Adv. Funct. Mater.* **2020**, *30*, 1903978.
- [33] D. Nahm, F. Weigl, N. Schaefer, A. Sancho, A. Frank, J. Groll, C. Villmann, H. - W. Schmidt, P. D. Dalton, R. Luxenhofer, *Mater. Horiz.* **2020**, *7*, 928.
- [34] A. C. Braun, M. Gutmann, T. Lühmann, L. Meinel, *J. Controlled Release* **2018**, *273*, 68.
- [35] A. H. St. Amant, D. Lemen, S. Florinas, S. Mao, C. Fazenbaker, H. Zhong, H. Wu, C. Gao, R. J. Christie, J. Read De Alaniz, *Bioconjugate Chem.* **2018**, *29*, 2406.
- [36] A. H. St. Amant, F. Huang, J. Lin, D. Lemen, C. Chakiath, S. Mao, C. Fazenbaker, H. Zhong, J. Harper, W. Xu, N. Patel, L. Adams, B. Vijayakrishnan, P. W. Howard, M. Marelli, H. Wu, C. Gao, J. Read De Alaniz, R. J. Christie, *Bioconjugate Chem.* **2019**, *30*, 2340.
- [37] M. Mees, E. Haladjova, D. Momekova, G. Momekov, P. S. Sheshtakova, C. B. Tsvetanov, R. Hoogenboom, S. Rangelov, *Biomacromolecules* **2016**, *17*, 3580.
- [38] M. A. Mees, R. Hoogenboom, *Polym. Chem.* **2018**, *9*, 4968.
- [39] R. Luxenhofer, *Nanomedicine* **2015**, *10*, 3109.
- [40] R. Luxenhofer, G. Sahay, A. Schulz, D. Alakhova, T. K. Bronich, R. Jordan, A. V. Kabanov, *J. Controlled Release* **2011**, *153*, 73.
- [41] F. C. Gaertner, R. Luxenhofer, B. Bleichert, R. Jordan, M. Essler, *J. Controlled Release* **2007**, *119*, 291.
- [42] L. Hahn, M. Maier, P. Stahlhut, M. Beudert, V. Flegler, S. Forster, A. Altmann, F. Töppke, K. Fischer, S. Seiffert, B. Böttcher, T. Lühmann, R. Luxenhofer, *ACS Appl. Mater. Interfaces* **2020**, *12*, 12445.
- [43] Lübtow, Mrlik, Hahn, Altmann, Beudert, Lühmann, Luxenhofer, *J. Funct. Biomater.* **2019**, *10*, 36.
- [44] M. Bauer, S. Schroeder, L. Tauhardt, K. Kempe, U. S. Schubert, D. Fischer, *J. Polym. Sci., Part A: Polym. Chem.* **2013**, *51*, 1816.
- [45] Y. Yu, Y. Zhang, J. A. Martin, I. T. Ozbolat, *J. Biomech. Eng.* **2013**, *135*, 91011.
- [46] J. Hauptstein, T. Böck, M. Bartolf-Kopp, L. Forster, P. Stahlhut, A. Nadernezhad, G. Blahetek, A. Zernecke-Madsen, R. Detsch, T. Jüngst, J. Groll, J. Teßmar, T. Blunk, *Adv. Healthcare Mater.* **2020**, *9*, 2000737.
- [47] B. L. Farrugia, K. Kempe, U. S. Schubert, R. Hoogenboom, T. R. Dargaville, *Biomacromolecules* **2013**, *14*, 2724.
- [48] K. Bott, Z. Upton, K. Schrobback, M. Ehrbar, J. A. Hubbell, M. P. Lutolf, S. C. Rizzi, *Biomaterials* **2010**, *31*, 8454.
- [49] C. M. Murphy, F. J. O'brien, *Cell Adhes. Migr.* **2010**, *4*, 377.
- [50] F. Geiger, D. Rüdiger, S. Zahler, H. Engelke, *PLoS One* **2019**, *14*, e0225215.
- [51] M. R. Arkenberg, D. M. Moore, C.-C. Lin, *Acta Biomater.* **2019**, *83*, 83.
- [52] D. Seliktar, A. H. Zisch, M. P. Lutolf, J. L. Wrana, J. A. Hubbell, *J. Biomed. Mater. Res. A* **2004**, *68A*, 704.
- [53] H. P. Wurst, K. Larbi, M. Herrmann, US20130052736, **2013**.
- [54] J. Ritzer, T. Lühmann, C. Rode, M. Pein-Hackelbusch, I. Immohr, U. Schedler, T. Thiele, S. Stübinger, B. V. Rechenberg, J. Waser-Althaus, F. Schlottig, M. Merli, H. Dawe, M. Karpíšek, R. Wyrwa, M. Schnabelrauch, L. Meinel, *Nat. Commun.* **2017**, *8*, 264.
- [55] A. C. Braun, M. Gutmann, T. D. Mueller, T. Lühmann, L. Meinel, *J. Controlled Release* **2018**, *279*, 17.
- [56] A. C. Braun, M. Gutmann, R. Ebert, F. Jakob, H. Gieseler, T. Lühmann, L. Meinel, *Pharm. Res.* **2017**, *34*, 58.
- [57] K. Dodt, S. Lamer, M. Drießen, S. Bölch, A. Schlosser, T. Lühmann, L. Meinel, *ACS Biomater. Sci. Eng.* **2020**, *6*, 5240.